Global and Planetary Change 109 (2013) 18–29

Contents lists available at ScienceDirect

Global and Planetary Change

journal homepage: www.elsevier.com/locate/gloplacha

Review paper

Up in smoke: A role for organic carbon feedbacks in Paleogene hyperthermals

Gabriel J. Bowen *

Department of Geology & Geophysics, University of Utah, Salt Lake City, UT 84112, USA
Global Change & Sustainability Center, University of Utah, Salt Lake City, UT 84112, USA

ARTICLE INFO

Article history:
Received 20 April 2013
Accepted 2 July 2013
Available online 8 July 2013

Keywords:
paleoclimate
PETM
hyperthermal
carbon isotope stratigraphy
carbon cycle
organic carbon
biogeochemistry
geochemical model

ABSTRACT

Sedimentary archives from the world's oceans and continents indicate that as the world warmed from the mild climate conditions of the mid-Paleocene to the extreme global warmth of the Early Eocene, a series of abrupt perturbations shifted the carbon isotope budget of the ocean/atmosphere/biosphere (exogenic) system. Consideration of the rates and magnitude of carbon isotope change, along with independent evidence for ocean acidification, dictates that these "hyperthermal" events involved the transfer of thousands of petagrams of reduced carbon to the actively cycling exogenic system. Careful study of stratigraphically resolved carbon isotope records spanning the hyperthermals, in particular the first and most prominent of them, the Paleocene–Eocene Thermal Maximum (PETM), has informed our understanding of carbon cycle perturbation during these events. Several important features of these records, however, remain difficult to explain with conventional ocean/atmosphere carbon cycle models, including divergence of carbon isotope records from marine and terrestrial systems, a prolonged interval of low $\delta^{13}C$ values during the 'body' of the PETM carbon isotope excursion (CIE), and rapid recovery of $\delta^{13}C$ values at the CIE termination. Here I use data from well-resolved, independently dated marine and terrestrial PETM carbon isotope records to characterize these distinctive and challenging features of the records and discuss their implications. I then propose a simple set of mechanisms, involving climatically-mediated increases in organic carbon respiration rates and CO_2-driven changes in photosynthetic ^{13}C discrimination triggered by an initial release of carbon from geological reservoirs, which produce patterns, magnitudes, and rates of carbon isotope change consistent with records from the event. If the proposed scenario is correct, it suggests that the land plants and soils may have first released, and then taken up, several thousand Pg of carbon during the early and late stages of the event, with concordant changes in rates of organic carbon burial in sediments. Full elaboration and rigorous evaluation of the proposed scenario will require additional work, but the initial results suggest that organic carbon feedbacks, similar in nature to those being explored in work on modern and future Earth systems, may have played a significant role in shaping global changes at the Paleocene–Eocene boundary.

Contents

* Tel.: +1 8015857925.
E-mail address: gabe.bowen@utah.edu.

0921-8181/$ – see front matter © 2013 Elsevier B.V. All rights reserved.
http://dx.doi.org/10.1016/j.gloplacha.2013.07.001

1. Introduction

Growing concern about the future trajectory of global carbon cycle and climate change in response to anthropogenic CO_2 emissions has motivated an intensive scientific focus on understanding future changes in terrestrial carbon storage. Land plants and soils on Earth today store at least 2000 Pg of organic carbon (Falkowski et al., 2000; Davidson and Janssens, 2006), most of it potentially reactive over timescales of months to centuries. Future changes in these stocks are expected to reflect a complex of forcing factors and internal controls, including temperature and CO_2 regulation of photosynthesis and respiration, changes in water and nutrient availability, and direct human land use decisions (Schimel, 1995). Despite growing process-level understanding and numerous theoretical and observational syntheses, substantial uncertainty remains regarding recent patterns and future projections of change in terrestrial carbon storage (Cox et al., 2000; Davidson and Janssens, 2006; Friedlingstein et al., 2006; Heimann and Reichstein, 2008; Huntzinger et al., 2012; King et al., 2012).

The geological record of global change may offer numerous opportunities to identify and characterize the gross effects and, potentially, mechanisms of change in terrestrial carbon storage during times of climatic change. In reality there are very few clear examples documenting such relationships, even for the recent glacial cycles of the Pleistocene (Adams and Woodward, 1990; Prentice and Fung, 1990; Bender, 2003). One potential example is the carbon cycle and climate perturbation at the Paleocene–Eocene boundary (the Paleocene–Eocene Thermal Maximum, PETM, 55.8 Ma), which took place during a geological interval of global "greenhouse" climate conditions and relatively high atmospheric CO_2 concentrations not dissimilar to those predicted for the late 21st and 22nd centuries (Friedlingstein et al., 2006). This event, and several subsequent "hyperthermal" events of smaller magnitude in the Early Eocene, featured coincidental global climatic warming and release of low-^{13}C carbon to the ocean/atmosphere/biosphere (exogenic) carbon cycle system. The source of the carbon remains a subject of debate, and viable hypotheses have been advanced that invoke release from terrestrial organic reservoirs (Kurtz et al., 2003; DeConto et al., 2012), seafloor gas hydrates (Dickens et al., 1995), or shallowly buried marine organic matter (Svensen et al., 2004). The PETM case offers compelling evidence for coupling of carbon redistribution between organic (reduced) and oxidized reservoirs with climatic change, but were terrestrial organic reservoirs a major contributor to the event? If so, what were the trigger, nature, and magnitude of this contribution?

Our most widely available and well-documented evidence for the PETM carbon cycle perturbation comes from carbon isotope records spanning the event, which document an abrupt, geologically short-lived, global negative carbon isotope excursion (CIE) affecting both marine and terrestrial carbon pools. Here I revisit the record of carbon isotope change through the PETM and highlight several distinctive features of this record that appear to be globally pervasive and require explanation in terms of the carbon budget of the exogenic system. I then propose a hypothesis invoking simple feedbacks in the terrestrial carbon cycle, based on assessments of modern biogeochemistry, that modulate carbon cycle and climatic change during the PETM through the 1) release (and subsequent uptake) of organic carbon from the land plants and soils and 2) reduction of organic carbon burial rates, both in response to initial PETM climate warming. I use a box model of the exogenic carbon cycle to demonstrate that the hypothesis can explain many of the otherwise enigmatic features of the PETM CIE. Although anecdotal evidence can be found in support of components of the proposed scenario, several key uncertainties and potential tests remain. I highlight these in hopes of motivating additional work to constrain whether the mechanisms proposed here, or related processes, can be convincingly linked to PETM global change, thus providing a strong evidence for changes in terrestrial carbon cycling as a contributor to past (and potentially future) climate change.

2. PETM records and age models

Relatively well-resolved PETM carbon isotope records are now available from a large number of marine and terrestrial sites worldwide (McInerney and Wing, 2011). These records have proven to be very useful for constraining the stratigraphic position of the event and correlating local environmental and biotic records to the global carbon cycle and climatic perturbation. The records have also clearly documented the global extent of the PETM carbon isotope perturbation, and could provide more detailed information on the pattern, pacing, and dynamics of carbon cycle change through the event. In this last regard, however, two major challenges have emerged. First, substantial changes in sediment accumulation rates during the PETM have been documented at many sites (Röhl et al., 2000, 2007; Farley and Eltgroth, 2003; Murphy et al., 2010), meaning that records which lack an independent, internal age model may not preserve accurate information on the time-evolution of carbon isotope ratios in the exogenic system. Although the development of internal age models for an event lasting 175–230 kyr (Murphy et al., 2007; Röhl et al., 2007) and occurring at 55.8 Ma (Westerhold et al., 2008) is challenging and sometimes prohibitive, independent models have now been developed for a number of sites through cyclostratigraphy or measurements of extraterrestrial ^{3}He dilution. Second, it has become increasingly clear that the carbon isotope change expressed in each "local" record is modulated relative to the "global" pattern by a complex of factors that likely varies from site to site and substrate to substrate (Bowen et al., 2004; McInerney and Wing, 2011). Major factors that have been identified include changes in substrate provenance (Sluijs and Dickens, 2012; Schneider-Mor and Bowen, 2013), time-averaging or truncation of records (Zachos et al., 2005; Schneider-Mor and Bowen, 2013), species assemblages (Gibbs et al., 2006a; Smith et al., 2007; Diefendorf et al., 2010), and environmentally-sensitive isotopic fractionation (Bowen et al., 2004; Schouten et al., 2007). As a result, patterns of change in local records must be considered in the context of external constraints and compared with data from other sites in order to infer regional or global patterns of carbon isotope change.

Here I consider well-resolved carbon isotope data representing isotopic changes in the surface ocean and atmosphere at five sites, each of which features one or more independent, internal age models for the PETM interval (Fig. 1). I use sediment core data from two pelagic marine sites, ODP sites 690 and 1266. Bulk carbonate records spanning the PETM are available for both sites (Bains et al., 1999; Zachos et al., 2005; Murphy et al., 2010), but the expression of the CIE in these records is known to be modulated by truncation associated with ocean acidification and shifting biological regimes (Bralower, 2002; Gibbs et al., 2006a, 2006b; McCarren et al., 2008). For site 690, additional data are available from analyses of the tests of surface, mixed-layer and bottom-dwelling foraminifera. Here I primarily consider data from single specimens of the thermocline-dwelling *Subbotina* sp. (Thomas et al., 2002). These single-specimen data are least likely to be biased by changes in time-averaging given that each measurement integrates over the lifetime of a single individual, and they eliminate potential effects of changing taxonomic assemblages. Thomas et al. also published single-specimen data from surface-dwelling *Acarinina* sp., but these records are strongly overprinted by short-term shifts early in the CIE that have been attributed to transient propagation of isotopically light carbon from the atmosphere through the surface ocean (Thomas et al., 2002). The *Subbotina* data preserve a well-resolved expression of the CIE that is intermediate to those recorded by *Acarinina* and bulk carbonate. Given this suite of considerations I take these data to be the most robust expression of large-scale changes in upper ocean $\delta^{13}C$ values for site 690 over $>10^3$ year timescales. The single-specimen data do not extend through the entire CIE, and to generate a complete record through the event I splice these data with bulk carbonate data (Bains et al., 1999), which display

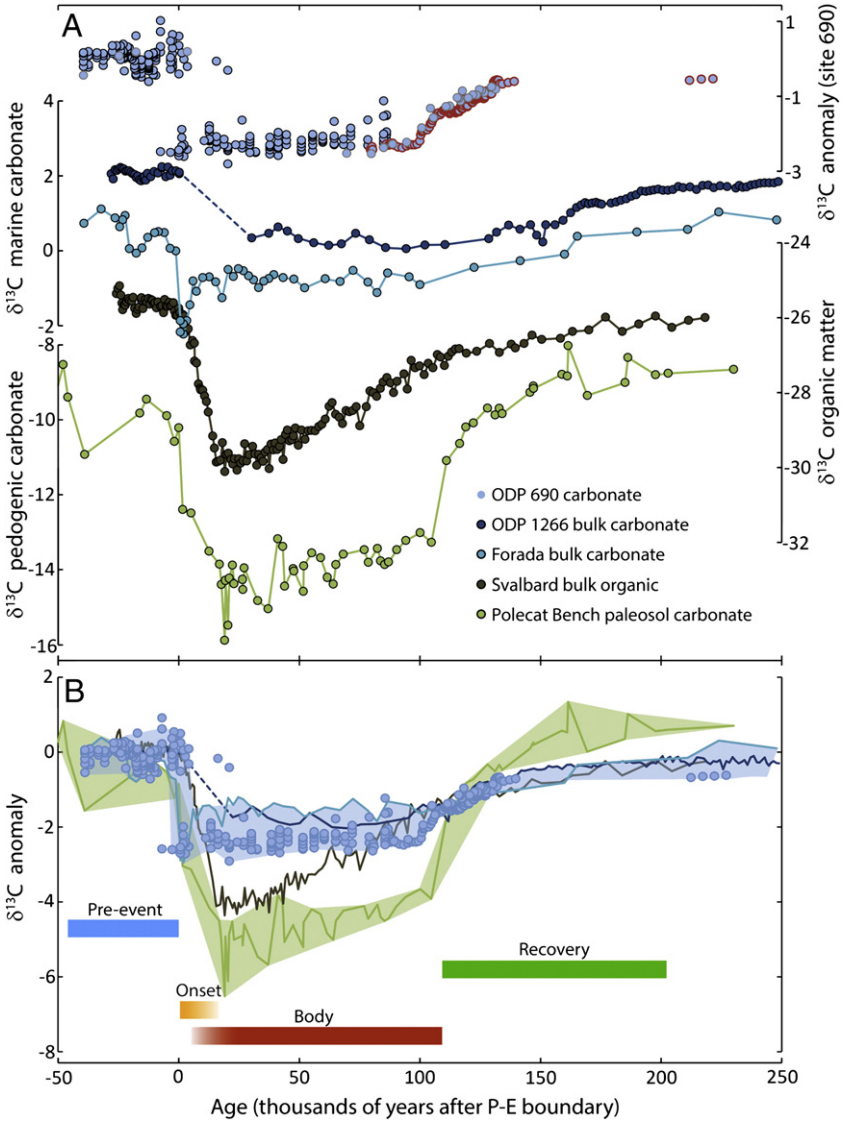

Fig. 1. PETM carbon isotope records from marine and terrestrial systems. A) Data from marine [ODP 690, southern ocean (Kennett and Stott, 1991; Bains et al., 1999; Thomas et al., 2002); ODP 1266, Walvis Ridge (Zachos et al., 2005; Murphy et al., 2010); Forada, Italy (Giusberti et al., 2007); Spitsbergen (Cui et al., 2011)] and terrestrial [Polecat Bench, WY (Bowen et al., 2001)] records. Values for each site represent a single substrate except for those from site 690, which represent single-specimen analyses of *Subbotina* sp. (black symbol outline), multi-specimen analyses of *Nuttalides trumpyi* (gray symbol outline), and bulk carbonate (red symbol outline). Records for site 690 are plotted as anomalies relative to each substrate's average value in the pre-CIE interval (here between 170.78 and 172 m below sea floor). Each record is plotted on an independent local age model (Farley and Eltgroth, 2003; Giusberti et al., 2007; Aziz et al., 2008; Murphy et al., 2010; Cui et al., 2011). For site 690 we use the low ^{3}He-flux calibration of Sluijs et al. (2007a). ODP 690 bulk carbonate data are known to be affected by changes in nanoplankton assemblages early in the event (Bralower, 2002), and are only plotted starting at 80 kyr after the P–E boundary. B) Generalized composite δ^{13}C anomaly fields for marine (blue field) and terrestrial (green field) systems. The marine field is drawn to enclose data (as anomalies relative to pre-CIE interval average values) from the marine sites, with the exception of the Spitsbergen data and four outlier single foram values from intervals in the site 690 record containing mixed excursion and non-excursion values. Sediment accumulation rates for site 1266 were linearly scaled by a factor of 0.74 in panel B to adjust the timing of the CIE recovery to be more consistent with the other records. The terrestrial field encloses data from the Polecat Bench local record.

patterns similar to available taxonomically-specific foram records from the latter part of the event (Fig. 1; Kennett and Stott, 1991).

I use published age models for both pelagic sites based on measured concentrations of ^{3}He (Farley and Eltgroth, 2003; Sluijs et al., 2007a; Murphy et al., 2010). These age models are qualitatively similar to each other, and to alternative cyclostratigraphic age models for these sites (Röhl et al., 2007), in that they indicate an oscillation between relatively slow accumulation rates during the early part of the CIE and rapid sediment accumulation late in the event. The ^{3}He age models differ in their estimates of the total duration of the carbon isotope perturbation, but the estimated duration of different internal features of the CIE is approximately proportional at the two sites (Murphy et al., 2010). If the major features of the CIE (i.e., onset, termination) reflect globally synchronous changes in the δ^{13}C values of exogenic carbon reservoirs, as suggested by the common pattern of change in these and other records (see below), this implies that the absolute accumulation rates estimated for one or both of the sites are inaccurate (Murphy et al., 2010; McInerney and Wing, 2011).

Internally dated carbon isotope records reflecting changing marine δ^{13}C values are also available at two marginal-marine sites. Bulk carbonate records from the Forada section in Italy have been dated by cyclostratigraphy (Giusberti et al., 2007). Although changes in local oceanographic and biological conditions may influence the CIE preserved in this record, it is less affected by carbonate dissolution during the initial stages of the event than are the records from the open-ocean pelagic sites. A carbon isotope record has also been produced at Forada based on analysis of terrestrial higher-plant leaf waxes (Tipple et al., 2011), but because of uncertainties in the degree

of time-averaging associated with transport of these biomarkers to the depositional site I do not consider this record here. A second cyclostratigraphically-calibrated record from marine-margin sediments at Spitsbergen is based on analysis of the $\delta^{13}C$ values of bulk sedimentary organic carbon (Cui et al., 2011). The authors argue, based primarily on context, that the preserved organic matter is dominantly of marine origin, but observed shifts in pristane/phytane ratios and global changes in sea level during the PETM (Sluijs et al., 2008a) suggest potential for changes in organic provenance through the record. Concerns have also been raised about the potential for significant time-averaging in this record associated with organic transport to the depositional site (Cui et al., 2012; Sluijs et al., 2012). As a result I primarily consider the Spitsbergen record in a qualitative sense.

I use data from a single terrestrial site, Polecat Bench, Wyoming, which has an associated cyclostratigraphic age model developed from patterns of color variation in pedogenically-modified floodplain sediments (Aziz et al., 2008). Carbon isotope data are available from both authigenic soil carbonate (Bowen et al., 2001; Bains et al., 2003) and bulk organic carbon (Magioncalda et al., 2004). I focus primarily on the $\delta^{13}C$ record of Bowen et al., which was generated from pedogenic carbonate collected in situ within freshly exposed paleosols. The pedogenic carbonate data provide a high-resolution record of changes in soil, plant, and presumably atmospheric CO_2 carbon isotope ratios, and because the pedogenic carbonates form in situ from soil CO_2 gas this record should be less susceptible than the bulk organic carbon record to time-averaging due to reworking or changing provenance. The CIE expression in the pedogenic carbonate record, however, was likely modulated by changes in local vegetation communities and ecosystem biogeochemistry during the PETM (Bowen et al., 2004; Smith et al., 2007). The Polecat Bench carbonate record is particularly notable for the large amplitude of the $\delta^{13}C$ shift it preserves, which is also characteristic, to varying degrees, of many other records derived from terrestrial substrates (McInerney and Wing, 2011).

These records are compared, expressed as anomalies relative to pre-CIE values for each site and substrate, in Fig. 1B. Each local record is plotted using its independent internal age model, with the only modification being that the site 1266 record has been linearly compressed by 26% to align the total CIE duration and pattern of change with the site 690 and Forada records. The marine and terrestrial records show a high degree of consistency in the overall pattern and pacing of carbon isotope change through the event. $\delta^{13}C$ values drop relatively abruptly at the onset of the event, though the apparent duration of the transition from pre-event to CIE values differs substantially between records, as has been previously discussed (e.g., Thomas et al., 2002; Cui et al., 2011). Following this initial drop all records show a prolonged interval of sustained, low $\delta^{13}C$ values. In most of the records this "body" phase of the event lasts for ~100,000 years (slightly longer in the un-adjusted 1266 record), with the Spitsbergen record (and the Forada leaf wax lipid record, not shown) preserving still distinct but somewhat shorter body intervals (~30,000 to 60,000 years). At the end of the body interval $\delta^{13}C$ values begin to recover toward values similar to those in the pre-event interval, with the recovery following a roughly exponential pattern in all records. The estimated duration of the recovery interval varies somewhat among records, but within ~100 kyr following the end of the CI body all records reach relatively stable post-excursion values.

Dickens et al. (1997) were the first to quantitatively model a scenario describing the evolution of global atmospheric and oceanic C isotopes through the PETM, and their work established the conceptual framework that is still applied to the problem today. The rapid (~10^4 years or less), large, and global perturbation of $\delta^{13}C$ values during the onset of the CIE cannot reasonably be explained by changes in carbon burial fluxes, and requires abrupt and catastrophic addition of ^{13}C-depleted C to the ocean/atmosphere system (Dickens et al., 1997). These authors argued for dissociation of oceanic methane hydrates as the primary source of the added carbon; since this initial proposition a large number of alterative or complementary C sources have been proposed (e.g., Kent et al., 2003; Kurtz et al., 2003; Svensen et al., 2004; Higgins and Schrag, 2006; DeConto et al., 2012). Whatever the source and form of carbon released, it would have been rapidly oxidized to CO_2 and propagated, over timescales of 10^3 years or less, through the ocean, atmosphere, and actively cycling terrestrial (plant and soil) carbon pools, driving the global carbon isotope excursion recorded in sedimentary archives. This shift in exogenic $\delta^{13}C$ values would establish an imbalance between the isotopic composition of carbon buried in rocks (which would change in parallel with changes in exogenic $\delta^{13}C$ values) and that entering the exogenic system through rock weathering and volcanism (which would not respond directly to changes in exogenic $\delta^{13}C$). After the release of ^{13}C-depleted carbon ceased, this imbalance would lead to the gradual dilution of excess ^{12}C and exponential decay of the carbon isotope perturbation at a rate related to the mean residence time of carbon in the exogenic system (Dickens et al., 1997; Dickens, 2001; Bowen and Zachos, 2010). This conceptual model adequately accounts for many of the first-order features seen in current, well-resolved, internally dated CIE records, but a number of features are also apparent that challenge our interpretation of the C isotope records in this context. In the next section I introduce three such challenges, related to the amplitude, prolonged body, and rapid recovery of the CIE. In Section 4 I suggest a simple modification to the Dickens et al. model that can help resolve the challenges through consideration of the active role of the terrestrial biosphere in global carbon cycle change.

3. Challenges to conventional models

3.1. Amplitude problem

The amplitude of the carbon isotope shift occurring at the onset of the PETM provides one of our best constraints on the source and amount of carbon released during the initiation of the event. Isotopic mass balance dictates that the CIE amplitude ($\Delta\delta^{13}C$) is a function of the amount (M_a) and isotopic composition ($\delta^{13}C_a$) of the carbon released to the exogenic system and the amount (M_i) and isotopic composition ($\delta^{13}C_i$) of carbon in the exogenic system prior to the event (see review in McInerney and Wing, 2011):

$$\Delta\delta^{13}C = \frac{\delta^{13}C_a M_a + \delta^{13}C_i M_i}{M_a + M_i} - \delta^{13}C_i.$$

Because the source of carbon (and hence its isotopic composition) is unknown, the CIE in and of itself cannot fully constrain the amount of carbon released, and several authors have conducted sensitivity tests to evaluate potential source/mass combinations that could account for the observed CIE, either through simple mass balance calculations or using numerical carbon cycle models (Pagani et al., 2006; Panchuk et al., 2008; Zeebe et al., 2009; McInerney and Wing, 2011). This latter approach allows additional constraints to be considered based on the pattern and extent of seafloor carbonate dissolution during the event, though both the interpretation of the dissolution data and the model-dependent changes in deep ocean saturation state have differed among studies (Panchuk et al., 2008; Zeebe et al., 2009; Cui et al., 2011). For any given estimate of $\Delta\delta^{13}C$ the required mass of carbon scales with the isotopic composition of the carbon source, such that estimates of M_a vary by a factor of 2 to 3 across a realistic range of possible carbon sources (Fig. 2).

Less attention has been given to the initial conditions of the exogenic carbon cycle prior to the event ($\delta^{13}C_i$ and M_i) (however, see Dickens, 2001). The isotopic composition can be constrained relatively well through measurements of marine carbonates, which characterize the $\delta^{13}C$ values of the largest carbon pool within the system (ocean deep water dissolved inorganic carbon). Empirical constraints on M_i

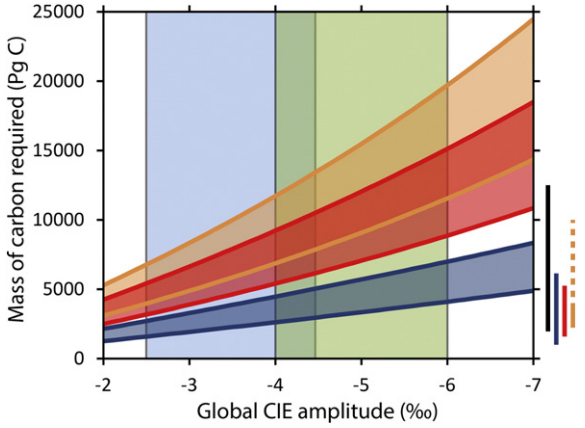

Fig. 2. Mass balance estimates for the initial PETM carbon isotope excursion [after Pagani et al. (2006) and McInerney and Wing (2011)]. Values represent the mass of carbon required to drive an instantaneous global exogenic C isotope decrease of the magnitude indicated on the x-axis, assuming carbon release from terrestrial organic matter ($\delta^{13}C = -25‰$, orange region), peatlands ($\delta^{13}C = -30‰$, red region), or methane hydrates ($\delta^{13}C = -60‰$, blue region). Calculations follow McInerney and Wing except that the mass of carbon stored in the late Paleocene ocean/atmosphere/biosphere system is varied between 31,770 Pg (lower curve for each scenario) and 54,190 Pg (upper curve), after Bowen and Zachos (2010). Blue and green vertical boxes show the range of $\delta^{13}C$ shifts observed during the CIE onset interval of the marine and terrestrial records (respectively) shown in Fig. 1. The vertical lines at the lower right indicate the estimated range of C release based on multiple interpretations of observed CCD shoaling (black line; Panchuk et al., 2008; Zeebe et al., 2009; Cui et al., 2011); estimated amount of frozen and free-gas methane associated with modern hydrates (blue line; Archer, 2007); simulated global permafrost C storage under a range of Paleogene climatic scenarios (red line; DeConto et al., 2012); and model-estimated range of early Paleogene terrestrial plant and soil carbon storage (orange line; Beerling, 2000), accounting for uncertainty in shallow sedimentary organic deposits that may have been susceptible to oxidation (dashed orange; Kurtz et al., 2003; Cui et al., 2011).

are limited, however. Bowen and Zachos (2010) attempted to integrate available information on late Paleocene marine cation concentrations and lysocline depth to estimate a potential range of values for M_i, but the analysis involved a number of untested assumptions and the constraints provided are not absolute. Applying the range of M_i estimates derived in that work to isotope mass balance calculations adds significant uncertainty to the possible range of M_a values associated with a given carbon source (Fig. 2). In particular, for the lower end of M_i estimates the released carbon mass required for any given carbon source is ~60% less than estimated in most previous calculations.

As significant, in terms of uncertainty imparted to the mass balance calculations, is uncertainty in the appropriate value for $\Delta\delta^{13}C$ (Fig. 2). The quantity of interest here is the mean, global amplitude of the PETM CIE averaged across the exogenic carbon cycle, but as Fig. 1 demonstrates there are substantial differences in the magnitude of the carbon isotope shift expressed in different records. In the past decade a large number of studies have highlighted this challenge and considered various mechanisms that might modulate the CIE amplitude recorded in various local records or classes of records (Bralower, 2002; Bowen et al., 2004; Schouten et al., 2007; Smith et al., 2007; Bowen and Bowen, 2008; Handley et al., 2008; McCarren et al., 2008; Diefendorf et al., 2010, 2011; Sluijs and Dickens, 2012; Schneider-Mor and Bowen, 2013; Schubert and Jahren, 2013). Beyond the variability apparent among individual local records, the data suggest systematic offsets in CIE amplitudes recorded in different environments — most notably between terrestrial and marine systems (e.g., Fig. 1; Bowen et al., 2004; McInerney and Wing, 2011). This heterogeneity in CIE amplitudes, and specifically the contrasting amplitudes recorded in terrestrial (approximately −4 to −6‰) and marine (approximately −2.5 to −4.5‰) systems, requires changes in carbon cycling and/or carbon isotope fractionation not currently incorporated in paleo-carbon cycle models applied to the PETM, which predict parallel evolution in marine, atmospheric and terrestrial $\delta^{13}C$ values over timescales of thousands of years (Fig. 3).

3.2. Body problem

Because carbon is continuously cycling between the exogenic system and rock reservoirs, a $\delta^{13}C$ perturbation caused by release of ^{13}C-depleted carbon to the exogenic system should begin to decay away as soon as carbon release ceases (see Section 2). This response is reflected in results from box models used to simulate the first-order effects of ^{13}C-depleted carbon release in a discrete pulse or pulses at the onset of the PETM: within approximately 1500 years following the cessation of carbon release the $\delta^{13}C$ values of carbon in all exogenic carbon reservoirs reach their minimum CIE values and begin a gradual, smooth increase toward "equilibrium" pre-event values (Fig. 3; e.g., Dickens et al., 1997; Dickens, 2003). However, the predicted pattern is a poor match for both marine and terrestrial PETM records, which feature a prolonged interval of sustained, low $\delta^{13}C$ values during the CIE "body" prior to the initiation of the recovery phase of the event (Bowen et al., 2006; McInerney and Wing, 2011).

The only possible explanation for the prolonged body of the CIE that has been explored in detail invokes a 'leaky' source of ^{13}C-depeleted carbon, such that the addition of isotopically light carbon to the exogenic system occurred not in a single discrete pulse but as a pulse followed by a prolonged, continuous trickle (Zeebe et al., 2009). The duration of the light carbon trickle was prescribed to be ~40 kyr in that study, but in reality must equal the duration of the CIE body (i.e., ~90 kyr for most of the internally-dated records compiled here).

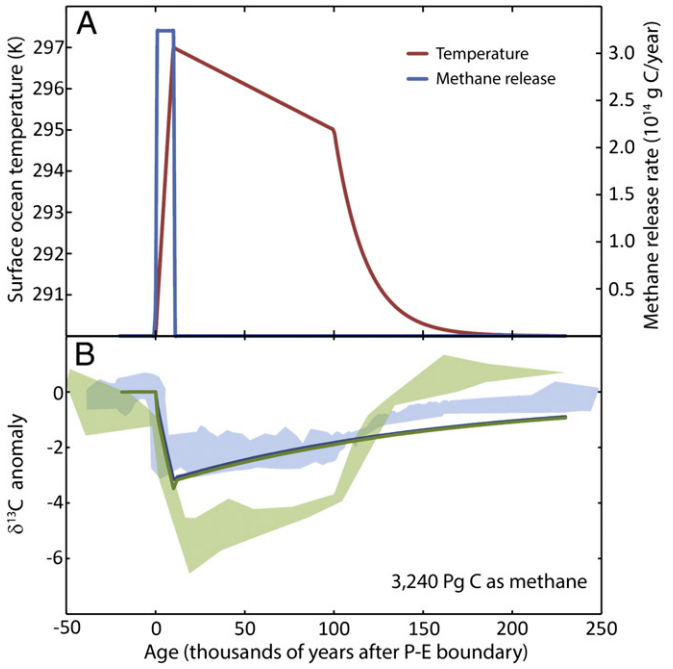

Fig. 3. Box model simulations of a single-pulse addition of ^{13}C-depleted carbon to an exogenic carbon cycle without organic feedbacks. A) Forcing applied in all carbon cycle box model experiments. Methane ($\delta^{13}C = -55‰$) is released directly to the atmosphere and rates are scaled in each experiment to achieve a deep ocean CIE amplitude of 3 ± 0.05‰; the values shown correspond to the control experiment shown in panel B. B) Simulated carbon isotope excursions in surface ocean (blue curve) and pedogenic (green curve) carbonates under a control scenario with 1) no changes in organic respiration 2) no changes in carbon isotope discrimination by land plants, and 3) a modern-sized terrestrial biosphere (2722 Pg C stored in plants and soils). Background color fields for surface ocean and terrestrial records are as in Fig. 1B. Here and elsewhere pedogenic carbonate $\delta^{13}C$ values are calculated assuming a fixed ^{13}C-enrichment of soil CO_2 relative to simulated terrestrial plant $\delta^{13}C$ values and temperature-dependent equilibrium fractionation between soil CO_2 and pedogenic carbonate.

One advantage of the leaky source model is that the prolonged addition of carbon to the ocean system slows the recovery of the lysocline and CCD, which records suggest remained suppressed throughout much of the CIE body, at least in the Atlantic ocean basin (Zachos et al., 2005; Kelly et al., 2010). This model, however, requires that added carbon was derived either from a single reservoir capable of a wide range of modal behaviors (i.e., long-term equilibrium before/after the event, short-lived catastrophic disequilibrium during the onset, and prolonged, steady, subtle disequilibrium during the CIE body) or multiple reservoirs with different characteristic timescales and rates of carbon release. Either scenario could be envisioned, but the challenge posed by the shape of the CIE body should motivate additional exploration and explication of mechanisms (Zeebe and Zachos, in press).

3.3. Recovery problem

At the termination of the CIE body $\delta^{13}C$ records show an inflection and accelerated rate of change toward higher values (Fig. 1). Within this recovery phase, $\delta^{13}C$ values follow an exponential trajectory from end-CIE body values to pseudo-equilibrium post-event values. Internal age models suggest that most marine records are significantly expanded within this interval, but there is some incongruence among age models in terms of the degree of expansion relative to the body of the event (Murphy et al., 2010; McInerney and Wing, 2011). Many marginal marine records are truncated by sea level regression during the recovery interval (e.g., Handley et al., 2008; John et al., 2008) and therefore not suitable for constraining changes in carbon cycling through the CIE recovery. Although continental records from other sites lack internal age control, several well-resolved records demonstrate a clear inflection in $\delta^{13}C$ values between the body and recovery phases that is congruent, in the depth domain, with the pattern expressed at Polecat Bench (Schmitz and Pujalte, 2003; Smith et al., 2007; Domingo et al., 2009).

The progression of values within the CIE recovery can be expressed as a progress variable in order to assess the fit of the exponential recovery model and estimate the recovery rate constant (Fig. 4; Cerling et al., 2007; Bowen and Zachos, 2010). As described by Bowen and Zachos (2010), the null model of carbon cycle recovery from the PETM via weathering feedbacks, carbonate carbon burial, and 'dilution' of the excess light carbon added during the PETM onset predicts that the recovery rate constant is related to the approximate mean residence time (MRT) of carbon in the exogenic system. These authors assessed the $\delta^{13}C$ recovery in the Polecat Bench and ODP site 690 records, and found that the recovery was consistent with MRT values of ~22,000 years, much lower than that estimated for the modern carbon cycle (~144,000 years) or any estimates derived from carbon cycle models of the Early Paleogene (Bowen and Zachos, 2010). Three possible scenarios were considered to explain this discrepancy: a less massive Early Paleogene exogenic carbon cycle, faster cycling rates to/from the crust, or rapid uptake (via burial in rocks or sequestration in one or more exogenic carbon pools) of ^{13}C-depeleted carbon during the recovery phase. Sensitivity testing suggested that only the latter of these mechanisms could plausibly explain the observed rapidity of the CIE recovery, consistent with inferences from box-model studies (Dickens, 2001) and Earth system model simulations tuned to reproduce the Spitsbergen record (Cui et al., 2011).

Rate estimates from each of the 5 sites compiled in Fig. 1 are consistent in suggesting that PETM $\delta^{13}C$ recovery proceeded at rates that were a factor of 2–6 faster than expected based on analogy to the modern carbon cycle (Fig. 4). Data from ODP site 1266, even without age model compression to align the duration of the CIE body with that seen in other records, closely match the previous result from site 690 and Polecat Bench and suggest recovery rates that are inconsistent with almost any plausible parameter space for the Early Paleogene carbon cycle. The other two new records from marine margin sites, Forada and Spitsbergen, show quite similar but slower recovery rates, consistent with an exogenic carbon cycle MRT of ~70,000 years (Fig. 4). This value lies well below the range of estimates for the modern carbon cycle, but could perhaps be consistent with some end-member scenarios for the Early Paleogene involving a less massive exogeneic carbon cycle (Fig. 2; Bowen and Zachos, 2010). Clearly both sets of records cannot be giving equivalent information on global carbon cycling rates and processes, suggesting that additional reconciliation of age models and record fidelity will be needed. Given that the Spitsbergen record may be affected by changes in organic provenance and/or time averaging (see above) and that alternative methods for defining precessional cyclicity at Forada have produced shorter durations for the recovery interval than that used here (Röhl et al., 2007), I consider the bulk of evidence to indicate that global exogenic $\delta^{13}C$ recovery from the PETM event was significantly faster than can be explained with conventional models of the event.

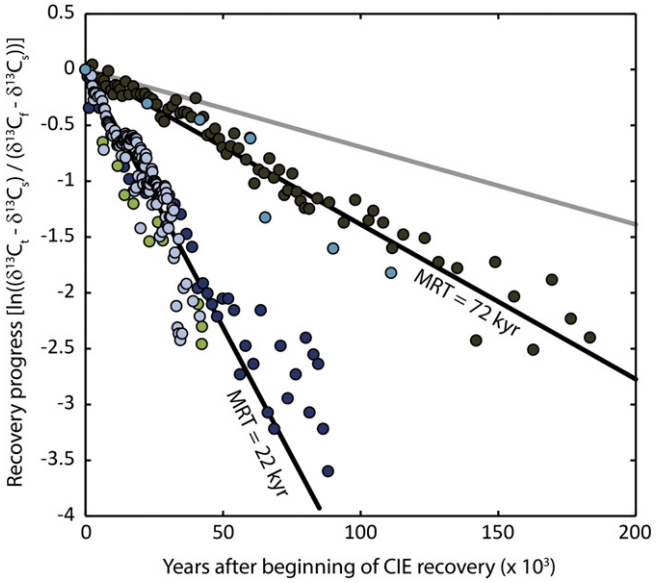

Fig. 4. Pattern and rate of exponential carbon isotope recovery during the CIE recovery interval for the five data sets plotted in Fig. 1A (after Bowen and Zachos, 2010). The metric plotted on the y axis gives the progress of the CIE recovery as a function of carbon isotope values at the current time (subscript t), the start of the CIE recovery (s) and the final post-excursion "equilibrium" value (f). Bold black lines give modeled values for an exponential CIE decay if the mean residence time (MRT) for carbon in the exogenic carbon cycle is 22 or 72 thousand years. The bold gray line gives the modeled pattern for a carbon MRT of 144 kyr, a central estimate for the modern carbon cycle (Bowen and Zachos, 2010). Other symbols are as in Fig. 1.

4. A role for organic carbon feedbacks?

4.1. Model framework

Changes in the carbon isotope composition and storage of terrestrial organic matter alter the distribution and fluxes of carbon isotopes within the carbon cycle through interaction with other exogenic reservoirs and mediation of carbon burial fluxes. I explore the potential role of such changes in governing the pattern of PETM exogenic $\delta^{13}C$ change using a simple carbon cycle box model. The model is derived from the work of Walker and Kasting (1992) and is similar in structure and function to models previously applied to the PETM (Dickens et al., 1997; Zeebe, 2012). It tracks the concentration of carbon, alkalinity, phosphorous and ^{13}C in two ocean reservoirs (representing global surface and deep water masses) and carbon and ^{13}C in one atmospheric

and one terrestrial biosphere reservoir. Ocean bathymetry is adjusted to reflect larger shelf areas in the Early Paleogene greenhouse and an interactive sediment model tracks inorganic carbon, ^{13}C and silicate burial in sea-floor sediments discretized into 15 water-depth-delimited bins. The sediment model is based on the study of Archer et al. (2002) and includes bioturbation (which is kept fixed here) and respiratory dissolution in 24 volume-conserving and 1 infinite (basal) sediment layer. Continental weathering feedbacks driven by changes in atmospheric CO_2 concentration modulate the fluxes of carbon, alkalinity and phosphorous to the surface ocean.

The model simulates the size and isotopic composition of the terrestrial biosphere as a function of global growth (photosynthesis), decay (respiration), and erosion (as dissolved and particulate organic carbon) fluxes. The feedbacks for which I conduct model sensitivity testing relate to these fluxes. Carbon dioxide fertilization of terrestrial photosynthesis is included in the model (Walker and Kasting, 1992), but this response is effectively saturated at the range of atmospheric CO_2 values simulated here and is not explored in detail. In this work, however, I incorporate a CO_2 effect on photosynthetic carbon isotope discrimination by land plants. Support for such an effect has been ambiguous based on experimental and observational data from low-CO_2 conditions, but recent work with high-CO_2 greenhouse experiments has helped to constrain the form and sensitivity of variation in photosynthetic discrimination by C_3 plants in response to CO_2 change (Schubert and Jahren, 2012). I adopt the hyperbolic relationship and sensitivity found in this work for discrimination between environmental $\delta^{13}CO_2$ and $\delta^{13}C$ of above-ground bulk biomass of *Raphanus sativus* to calculate changes in discrimination between atmospheric CO_2 and new organic matter added to the model's terrestrial biosphere.

The second feedback tested in this work involves sensitivity of organic matter respiration rates to environmental temperature. Decades of work have demonstrated that respiration rates in a wide range of systems generally increase with increasing temperature, as commonly described by a Q10 factor (where Q10 is the relative change in respiration rate in response to a 10 °C increase in temperature; see Fang and Moncrieff, 2001). Here I test the effect of adopting a fixed Q10 value of 3, which is within the range of values reported for modern ecosystems (Fang and Moncrieff, 2001) but approximately a factor of 2 higher than current estimates of the global average value (Zhou et al., 2009; Mahecha et al., 2010). This scenario is not intended to represent a realistic direct biochemical response to temperature warming but rather to investigate an endmember scenario for net effective response to climate change during the PETM — indeed site-specific evidence exists for strong biosphere responses to other environmental forcers (e.g., changing precipitation regimes) that accompanied PETM climate warming (Wing et al., 2003, 2005; Bowen and Bowen, 2008). The Q10 factor was applied to scale organic respiration rates for the terrestrial biosphere and for marine sedimentary organic carbon burial. In the first case, enhanced respiration increases the fraction of terrestrial organic carbon respired to the atmosphere per unit time. In the second case enhanced respiration reduces the fraction of organic carbon reaching seafloor sediments which is ultimately buried.

The model version used here was tuned to achieve a high-pCO_2 (900 ppmv) Early Paleogene background state by adjusting setpoints for the rock weathering fluxes. The tuned state has a relatively massive exogenic carbon cycle containing 52,500 Pg of carbon, near the upper end of estimates shown in Fig. 2 (Bowen and Zachos, 2010), with a terrestrial biosphere reservoir containing 2722 Pg of carbon ("modern biosphere", similar to the modern value). A second tuned state with a substantially larger biospheric carbon reservoir (6818 Pg, "big biosphere") was also tested to evaluate the potential sensitivity of the system to more widespread vegetation and organic-rich surficial deposits estimated for the Early Paleogene (Beerling, 2000; Kurtz et al., 2003). Given the simplicity of the ocean model I have not attempted to precisely match observed Early Paleogene CCD or lysocline depths, and the somewhat deeper-than observed tuned model lysocline depth of 4.5 km along with the relatively massive exogenic carbon cycle contribute to making the model less sensitive to applied perturbations than would be the case for a leaner tuning. In this sense, the results here can be considered conservative with respect to the spectrum of possible responses.

Four optimized model scenarios are reported here that evaluate responses to a transient ^{13}C-depleted carbon injection, with and without biosphere feedbacks (carbon isotope fractionation and respiration), for modern and big Early Paleogene biosphere stock sizes. All simulations were driven with a common set of prescribed temperature change and carbon release forcings (Fig. 3). Isotopically light (−55‰) carbon was added directly to the atmosphere in a single 10,000 year pulse to simulate an idealized release of carbon from a methane hydrate reservoir. In each scenario the amount of carbon released was scaled to achieve a uniform CIE amplitude of 3‰ in the deep ocean reservoir. The total amount of carbon required varied from 1560 to 3480 Pg depending on the scenario. In order to isolate first-order carbon cycle responses to observed PETM environmental change, the model was forced with an idealized temperature change function (Fig. 3) based on marine records (Zachos et al., 2003, 2006). The temperature anomaly was applied across all model components to drive parallel temperature changes of equal amplitude.

4.2. Organic feedbacks

Carbon isotope change in the control scenario (modern biosphere, no biosphere feedbacks) closely mimics that seen in previous box model experiments simulating a discrete pulse of light carbon injection followed by relaxation of the carbon cycle with or without silicate weathering feedbacks (Fig. 3; Dickens et al., 1997; Dickens, 2003). The mass of carbon required to obtain the target CIE amplitude in the relatively massive exogenic carbon cycle simulated here (3240 Pg) is near the high end of values simulated in previous studies (Dickens et al., 1997; Zeebe et al., 2009), and although it lies within the range of uncertainty for C storage in Early Paleogene gas hydrate reservoirs (Buffett and Archer, 2004; Archer, 2007; Dickens, 2011) this scenario would require substantial depletion (1/2 or more) of a relatively large hydrate reservoir. More problematically, however, the model-simulated changes in $\delta^{13}C$ fail to reproduce any of the distinctive features of the CIE described in Section 3. With the exception of short-lived ($\leq 10^3$ years) offsets as the released carbon propagates through the exogenic system and offsets between carbon-bearing phases related to temperature-driven changes in equilibrium fractionation factors (not shown), the $\delta^{13}C$ values of the marine, atmosphere and biosphere reservoirs evolve in parallel throughout the event. Carbon isotope recovery commences immediately following the cessation of carbon release, and the system evolves smoothly toward baseline values, with an apparent MRT for exogenic carbon of ~100,000 years (calculated from the first 100,000 years of modeled recovery interval results, analogous to Fig. 4).

Simulations that include terrestrial biosphere feedbacks predict substantially different patterns of $\delta^{13}C$ change in response to the prescribed forcing (Fig. 5). The mass of (methane) carbon release required to achieve the target 3‰ deep ocean CIE is lower than in the control scenario by 25% (modern biosphere) to 50% (big biosphere). This result is largely driven by the release of isotopically light carbon from terrestrial biospheric stocks in response to enhanced respiration at higher temperatures (Fig. 6D), which contributes an additional 1200 to 3000 Pg of carbon to the ocean/atmosphere system as a feedback on PETM climate warming. Although the boundary conditions (e.g., biosphere stock size) and scaling of this feedback are poorly constrained, the model results highlight the potential for cascading feedbacks to release carbon from multiple reservoirs during the event, with significant implications for the use of mass-balance to constrain the amount of carbon release from a 'master' or 'triggering' reservoir.

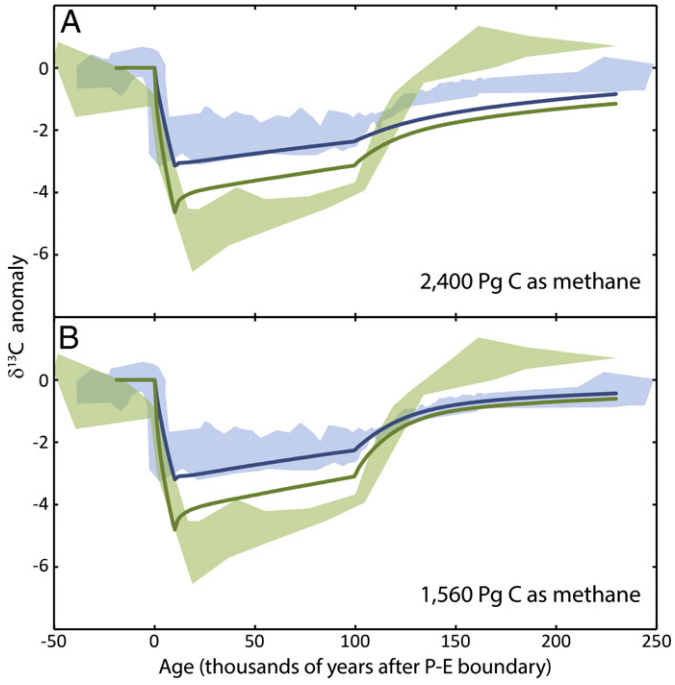

Fig. 5. Simulated carbon isotope excursions under two organic carbon feedback scenarios, with symbols as in Fig. 3B. A) Organic respiration feedback and CO_2-driven changes in land plant C isotope discrimination, modern sized pre-event terrestrial biosphere. B) Organic respiration feedback and CO_2-driven changes in land plant C isotope discrimination, 'big' pre-event terrestrial biosphere (6818 Pg C in plants and soils). Forcing in both scenarios follows Fig. 3A, with the total mass of C released as methane indicated here.

The feedback-enabled simulations, which incorporate variable carbon isotope discrimination by land plants, predict divergence between the $\delta^{13}C$ values of marine and terrestrial substrates within the body of the CIE (Fig. 5). This effect is a direct result of increases in atmospheric pCO_2 during the event (Fig. 6A), which force an increase in photosynthetic ^{13}C-discrimination of between 1.0 and 1.5‰. The total magnitude of this divergence is less than that separating the marine and Polecat Bench paleosol carbonate $\delta^{13}C$ records during the CIE body (Fig. 5), but is similar to the divergence between marine records and land plant biomarker carbon isotope records from several sites (Smith et al., 2007; Handley et al., 2008). In theory this congruence could provide a constraint on the magnitude of atmospheric pCO_2 change during the PETM (Schubert and Jahren, 2013), here estimated to be between 600 and 950 ppmv, with the caveat that the result is sensitive to the assumed background Early Paleogene pCO_2 level. The divergence is greatest during a short-lived (~15,000 year) interval surrounding the cessation of the pulsed light-carbon release (Fig. 5), when ocean acidification temporarily increases the fraction of the added carbon residing in the atmosphere. This pattern is consistent with that observed in high-resolution terrestrial records (Fig. 1A) that show a discrete interval of very low $\delta^{13}C$ values at the beginning of the PETM body.

Perhaps the most striking impact of the imposed organic carbon feedbacks on modeled PETM carbon isotope timeseries, however, is that in the absence of other external factors (e.g., leaky carbon reservoirs) the simulated feedbacks can drive both the prolonged, semi-stable body and abrupt, rapid CIE recovery that are documented in the proxy records but missing from the control simulation (Fig. 5). The results vary somewhat with assumed boundary conditions, but in both the modern and big biosphere simulations the rate of $\delta^{13}C$ recovery during the CIE body is much slower than in the control case (e.g., surface ocean $\delta^{13}C$ increases by <0.8‰, vs. 1.3‰ in the control simulation, during model years 20,000–100,000). The reduced rate of carbon isotope change during this interval results from a decrease in the simulated rates of organic carbon burial in sedimentary rocks (Fig. 6F), driven both by reduced burial efficiency (enhanced respiration according to the Q10 function) and reduced supply of particulate organic carbon from a smaller terrestrial biosphere. This effect is partially offset by enhanced marine export production, induced by a growth in marine PO_4^{3-} concentrations as less phosphate is buried with organic matter (Fig. 6E).

Once the imposed temperature forcing is relaxed (model year 100,000) global exogenic $\delta^{13}C$ values begin to rapidly recover toward post-event values. Apparent exogenic carbon cycle MRT values, calculated from the first 100,000 years of recovery interval $\delta^{13}C$ values, range from 34,000 to 49,000 years depending on the assumed background mass of the terrestrial biosphere (with shorter MRT values for larger biosphere size), within the range of values indicated by observational data (Fig. 4). The accelerated CIE recovery largely reflects uptake of carbon by the terrestrial biosphere as temperatures cool,

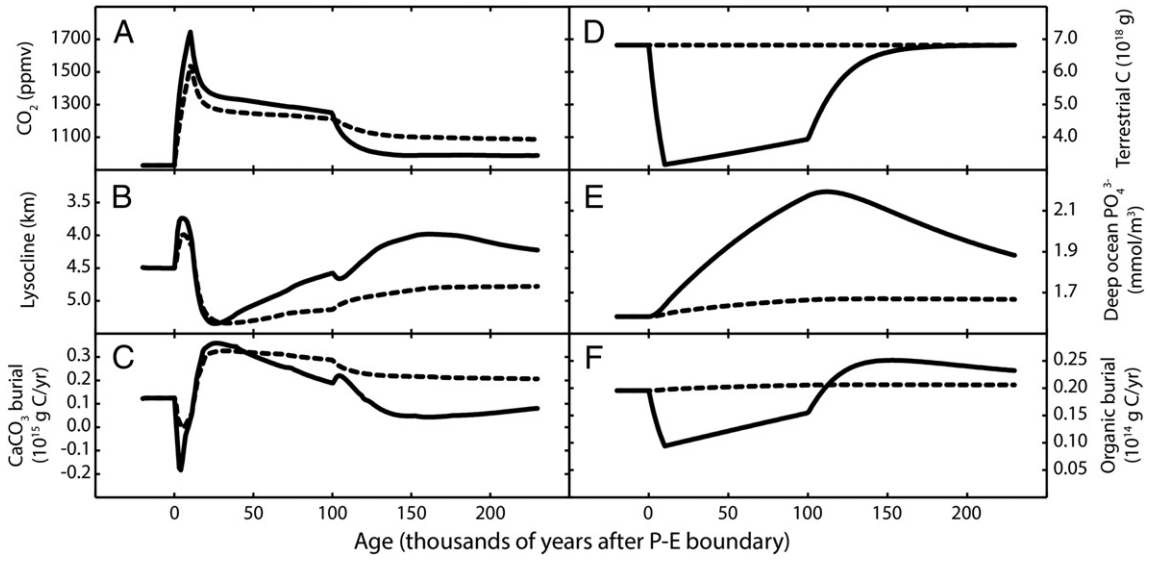

Fig. 6. Model-simulated biogeochemical responses to C release with (solid line) or without (dashed line) organic C feedbacks. Both simulations represent the release of C (1560 Pg with feedbacks, 3480 Pg without feedbacks) as methane and climate warming, as in Fig. 4, into an exogenic carbon cycle with a 'big' pre-event terrestrial biosphere (6818 Pg C in plants and soils). A) Atmospheric CO_2 concentration, B) calcite lysocline depth, C) net global marine carbonate burial rate, D) terrestrial organic carbon storage, E) deep ocean phosphate concentration, and F) global organic carbon burial rate.

respiration rates decrease, and the size of this stock rebounds to pre-event levels (Fig. 6D). This effect is reinforced by modest increases in sedimentary organic carbon burial relative to the control case, driven by increased marine phosphate levels and productivity (Fig. 6E and F).

5. Discussion

The simulations presented above suggest that a simple set of feedbacks involving organic carbon respiration and photosynthetic carbon isotope fractionation could explain several salient features of the PETM CIE that are not otherwise consistent with models of carbon cycle response to a discrete, short-lived carbon injection. The model predicts that by modulating both the storage and burial rates of organic carbon, climatically-driven changes in respiration could have amplified an initial pulsed carbon release from methane hydrates, thermogenic methane, or another source external to the ocean–atmosphere–biosphere system. For the methane source investigated here, the additional release of carbon from the terrestrial biosphere increased the transient rise in atmospheric pCO_2 simulated during the event (Fig. 6A), somewhat reducing the previously established mismatch between potential radiative forcing by CO_2 and climate warming observed during the PETM (Zeebe et al., 2009). At the same time, the terrestrial biosphere acted as a secondary source of isotopically light carbon to the ocean/atmosphere system in this scenario, reducing the amount of carbon required from methane hydrates or another exotic source in order to trigger the event. At the termination of the event, the same feedback mechanisms could have accelerated recovery of both exogenic $\delta^{13}C$ values and atmospheric pCO_2, pulling the carbon cycle and climate system out of the perturbed state characterizing the body of the PETM.

Within the proposed model the terrestrial biosphere effectively acts as a carbon cycle capacitor, in the sense of Dickens (2003): storing, releasing, and re-charging its stock of reduced carbon through the course of the PETM. The proposed model invokes carbon release from this capacitor as a first-order feedback responding to externally-induced warming (e.g., from released hydrates), along the lines of envisioned future carbon cycle feedbacks triggered by anthropogenic fossil fuel burning (Friedlingstein et al., 2006; Heimann and Reichstein, 2008; Zhou et al., 2009). The proposed organic respiration scenario has at least two key differences that distinguish it from an equivalent scenario involving methane hydrate release alone, and which might provide a basis for further testing of the model. The first is the nature of the connection between organic carbon respiration rates and burial of organic carbon in the lithosphere. Within the modeled scenario, the smaller standing stock of terrestrial organic carbon and higher rates of respiration in sea floor sediments reduce the flux of ^{13}C-depleted carbon to rocks during the event, which sustains the low exogenic $\delta^{13}C$ values that comprise the CIE body. Thermal destabilization of hydrates and delayed re-charge of a hydrate capacitor would not in and of itself lead to the same effect, meaning that continued, prolonged release of hydrates at a wide range of different release rates is required to explain the CIE body (Dickens, 2003; Zeebe et al., 2009). The second distinguishing factor is that, unlike for hydrates, constraints exist, from Quaternary paleoecology, on rates of change in terrestrial ecosystems and carbon storage (e.g., Jackson and Overpeck, 2000; Jobbagy and Jackson, 2000; Trumbore, 2000) that indicate that substantial changes in carbon stocks are plausible on 10^4–10^5 year timescales. Rapid regrowth of terrestrial carbon stocks over these timescales is required by the proposed model to replicate the CIE recovery, and although a similar isotopic effect could arise from regrowth of a methane hydrate capacitor it is not clear that the rates of hydrate accumulation are sufficient to explain the observed pattern of CIE termination (Dickens, 2003).

The model proposed here, while admittedly crude, exhibits first-order consistency with a number of documented features of the PETM. The simulated transient decrease in terrestrial organic carbon storage and burial rates of organic carbon in rocks is consistent with the limited evidence available from several continental sedimentary sequences that preserve more oxidized deposits within the body of the PETM than below or above (Wing et al., 2003; Kraus and Riggins, 2007; Domingo et al., 2009), and with paleoecological reconstructions at some mid-latitude sites that suggest more open, perhaps less productive ecosystems during the PETM (Wing et al., 2005; Bowen and Bowen, 2008; McInerney and Wing, 2011). In many cases these changes have been attributed to alteration of the water cycle during the PETM, rather than to temperature effects. Although the thermally-driven respiration effect provides a first-order link between climatic perturbation and organic carbon cycling that can be incorporated in the simple model used here, it is perhaps better considered as an idealized representation of a complex of climate-driven responses that might occur in a warming, more seasonal, and more extreme climate system.

Several studies of continental margin sediments have made the case for elevated rates of organic burial in such settings during the PETM body (John et al., 2008; Sluijs et al., 2008b), which is not immediately consistent with the modeled scenario. Burial rate comparisons given in these studies, however, are subject to significant uncertainties associated with unconstrained changes in sediment accumulation rates within the PETM, uneven comparison of short-term (PETM, $<10^5$ year) and long-term (background, $>10^6$ year) rates (Sadler, 1981), and potential changes in organic provenance during the event (Sluijs and Dickens, 2012; Schneider-Mor and Bowen, 2013). In other marginal marine settings, enhanced organic carbon concentrations appear to correlate with the later stages (recovery) of the event (Schulte et al., 2011), which is more consistent with the pattern of change simulated here. Given the importance of continental margin environments as a sink for organic carbon in the modern (Muller-Karger et al., 2005), the timing and magnitude of PETM changes in organic carbon burial in such settings deserve additional attention.

One significant discrepancy between the simulations conducted here and the observational record relates to the pattern of changes in lysocline depth. The model simulations reproduce the general pattern of changes in ocean deepwater carbonate saturation known from pelagic records, with an initial shoaling of the lysocline and CCD in response to carbon addition and subsequent over-compensation. Data from most pelagic sites show that the resumption of high-$CaCO_3$ sediment accumulation in the deep ocean, associated with deepening and over-compensation of the lysocline, does not occur until the recovery interval of the event (Zachos et al., 2005; Kelly et al., 2010). In contrast, the model used here generates shoaling lasting only ~20,000 years, followed immediately by deepening, over-compensation and enhanced $CaCO_3$ burial during the body of the CIE (Fig. 6B and C). This pattern can to some degree be attributed to the simplicity of the ocean model used in this work. The two-box ocean model, run with a relatively deep starting lysocline depth and without any changes in sediment bioturbation during the PETM (Panchuk et al., 2008; Nicolo et al., 2010), exposes a huge inventory of sea-floor sediment $CaCO_3$ to rapid dissolution, limiting the magnitude and duration of lysocline changes in the model. Previous work with box models incorporating a larger number of ocean reservoirs has suggested that it is difficult to sustain lysocline shoaling throughout the PETM body without continued addition of carbon to the ocean/atmosphere system throughout the event (Zeebe et al., 2009), but further work will be required to more rigorously evaluate this result in the context of the scenario modeled here and given reconstructed changes in bioturbation, which were not evaluated in the cited study.

The model presented here is sensitive to the assumed background state of the terrestrial biosphere. In a scenario wherein the amount of carbon stored in living plants and soils is approximately equal to that existing today, the simulated organic carbon feedbacks are significant

but not adequate to fully account for the observed pattern of land and ocean $\delta^{13}C$ change (in particular the rapid $\delta^{13}C$ recovery), despite modeled changes in biospheric carbon storage approaching ~50% of the pre-event value. In contrast, applying the same scenario assuming a larger and potentially realistic late Paleocene terrestrial carbon stock (~2.5 times modern) produces a $\delta^{13}C$ response that is largely consistent with the observed pattern and rates of changes. Currently, estimates of early Paleogene terrestrial carbon storage are constrained only by a handful of Earth system model simulations (Beerling, 2000; Beerling et al., 2011). An opportunity exists to refine our understanding of this important carbon cycle parameter for Early Paleogene greenhouse climate conditions that may be relevant to future climate states. Better estimates of the magnitude of carbon storage in the Early Paleogene terrestrial biosphere may also be relevant to evaluating other hypothesized links between the global carbon cycle and terrestrial biogeochemical processes, such as multi-million year trends in Paleocene and Eocene exogenic carbon isotope budgets (Oberhansli and Perch-Nielsen, 1990; Kurtz et al., 2003) and non-CO_2 greenhouse gas forcing of Paleogene climate (Beerling et al., 2011).

The hypothesis advanced here describes how PETM temperature (and perhaps other climatic) changes may have induced organic carbon feedbacks that contributed significantly to PETM global change. However, the simulations I have conducted are forced by prescribed methane release and temperature change functions, and thus do not address or explain the triggering of the event or the two-way coupling between carbon cycle and climate systems throughout the various phases of the event. A comprehensive and self-consistent explanation for the PETM will require such a model. A number of plausible scenarios for PETM initiation via external forcing or threshold-crossing events have already been advanced (e.g., Svensen et al., 2004; Sluijs et al., 2007b), and could be invoked here. PETM temperatures applied to force my model reflect the relatively large (5–7 °C) changes observed in proxy records. The pattern of atmospheric pCO_2 change produced by the models incorporating organic carbon feedbacks (Fig. 6A) is broadly consistent with the pattern of temperature change observed, suggesting that biospheric carbon feedbacks and associated pCO_2 change could have helped structure the pattern of PETM climate change. As in previous modeling efforts, however, I find that the observed magnitude of pCO_2 change, even in the most extreme scenarios considered here, is insufficient to explain PETM climate warming assuming any 'reasonable' sensitivity of global temperatures to a doubling of atmospheric CO_2 concentration (Pagani et al., 2006; Zeebe et al., 2009; McInerney and Wing, 2011), implying the need for additional work exploring indirect mechanisms of climate change amplification during the event. Finally, the form of the exogenic $\delta^{13}C$ and temperature records, and the scenarios modeled here and elsewhere (Zeebe et al., 2009), imply a discrete change in the global carbon/climate system at the transition between the PETM body and recovery. Initiation of the CIE recovery interval requires a change in exogenic carbon isotope mass balance, which is here accomplished largely through rapid re-growth of terrestrial organic carbon stocks. Relatively little attention has been given to this apparently discrete transition to the PETM recovery state, but understanding the external forcing or internal thresholds involved will be important in assessing and projecting potential long-term (10^5 year) responses of the Earth system to massive carbon cycle perturbation.

6. Conclusion

Carbon isotope records spanning the PETM provide important constraints on the perturbation of the global carbon cycle during this event, but several key features of high-resolution, internally dated records are challenging to explain with conventional carbon cycle models. The work presented here describes and evaluates a new hypothesis that invokes climatically-driven organic carbon feedbacks, triggered by an initial geological carbon release, as a significant contributor to PETM carbon cycle and climatic change. The respiration feedback modeled here can, by altering the storage of carbon in terrestrial plants and soils and the burial rates of carbon in sedimentary rocks, partially or fully account for several distinctive features of the PETM CIE, including the prolonged CIE body and rapid $\delta^{13}C$ recovery. Together with a recently advanced mechanism relating land plant carbon isotope fractionation to pCO_2 (Schubert and Jahren, 2012, 2013), these responses make the modeled scenario consistent with most aspects of the marine and terrestrial carbon isotope records compiled here. Several aspects of the scenario require further testing and evaluation relative to geological data, and a fully independent model evaluating coupling of the carbon cycle and climate mechanisms suggested here is needed. This work, however, suggests that the PETM carbon isotope record may indicate a significant role for changes in terrestrial biogeochemistry in governing global change during this major geological climate change event, highlighting the potential for equivalent changes to influence the trajectory of future global change.

Acknowledgments

The ideas underlying this work emerged through discussions with many individuals, and in particular I'd like to thank Scott Wing, Matt Huber, Clement Bataille, and Bianca Maibauer for discussion and inspiration. This work was supported by U.S. National Science Foundation grants OCE-0902882 and EAR-1261312.

References

Adams, J., Woodward, F., 1990. Increases in terrestrial carbon storage from the Last Glacial Maximum to the present. Nature 348 (6303), 711–714.
Archer, D., 2007. Methane hydrate stability and anthropogenic climate change. Biogeosciences 4, 521–544.
Archer, D.E., Morford, J.L., Emerson, S.R., 2002. A model of suboxic sedimentary diagenesis suitable for automatic tuning and gridded global domains. Global Biogeochemical Cycles 16. http://dx.doi.org/10.1029/2000GB001288.
Aziz, H.A., et al., 2008. Astronomical climate control on paleosol stacking patterns in the upper Paleocene–lower Eocene Willwood Formation, Bighorn Basin, Wyoming. Geology 36 (7), 531–534.
Bains, S., Corfield, R.M., Norris, R.D., 1999. Mechanisms of climate warming at the end of the Paleocene. Science 285 (5428), 724–727.
Bains, S., et al., 2003. Marine–terrestrial linkages at the Paleocene–Eocene boundary. In: Wing, S.L., Gingerich, P.D., Schmitz, B., Thomas, E. (Eds.), Causes and Consequences of Globally Warm Climates in the Early Paleogene. Geological Society of America Special Paper, 369. Geological Society of America, Boulder, Colorado, pp. 1–9.
Beerling, D.J., 2000. Increased terrestrial carbon storage across the Palaeocene–Eocene boundary. Palaeogeography, Palaeoclimatology, Palaeoecology 161, 395–405.
Beerling, D.J., Fox, A., Stevenson, D.S., Valdes, P.J., 2011. Enhanced chemistry-climate feedbacks in past greenhouse worlds. Proceedings of the National Academy of Sciences 108 (24), 9770–9775.
Bender, M., 2003. Climate–biosphere interactions on glacial–interglacial timescales. Global Biogeochemical Cycles 17, 1082. http://dx.doi.org/10.1029/2002GB001932.
Bowen, G.J., Bowen, B.B., 2008. Mechanisms of PETM global change constrained by a new record from central Utah. Geology 36 (5), 379–382.
Bowen, G.J., Zachos, J.C., 2010. Rapid carbon sequestration at the termination of the Paleocene–Eocene Thermal Maximum. Nature Geoscience 3, 866–869.
Bowen, G.J., et al., 2001. Refined isotope stratigraphy across the continental Paleocene–Eocene boundary on Polecat Bench in the Northern Bighorn Basin. In: Gingerich, P.D. (Ed.), Paleocene–Eocene Stratigraphy and Biotic Change in the Bighorn and Clarks Fork Basins, Wyoming. University of Michigan Museum of Paleontology, Ann Arbor, MI, pp. 73–88.
Bowen, G.J., Beerling, D.J., Koch, P.L., Zachos, J.C., Quattlebaum, T., 2004. A humid climate state during the Palaeocene–Eocene Thermal Maximum. Nature 432, 495–499.
Bowen, G.J., et al., 2006. Eocene hyperthermal event offers insight into greenhouse warming. Eos 87 (17), 165–169.
Bralower, T.J., 2002. Evidence of surface water oligotrophy during the Paleocene–Eocene Thermal Maximum: nannofossil assemblage data from Ocean Drilling Program Site 690, Maud Rise, Weddell Sea. Paleoceanography 17 (2), 1023. http://dx.doi.org/10.1029/2001PA000662.
Buffett, B., Archer, D., 2004. Global inventory of methane clathrate: sensitivity to changes in the deep ocean. Earth and Planetary Science Letters 227, 185–199.
Cerling, T.E., Bowen, G.J., Ehleringer, J.R., Sponheimer, M., 2007. The reaction progress variable and isotope turnover in biological systems. In: Dawson, T.E., Siegwolf, R. (Eds.), Stable Isotopes as Indicators of Ecological Change. Elsevier, Amsterdam, pp. 163–172.
Cox, P.M., Betts, R.A., Jones, C.D., Spall, S.A., Totterdell, I.J., 2000. Acceleration of global warming due to carbon-cycle feedbacks in a coupled climate model. Nature 408 (6809), 184–187.

Cui, Y., et al., 2011. Slow release of fossil carbon during the Palaeocene–Eocene Thermal Maximum. Nature Geoscience. Macmillan Publishers Limited.

Cui, Y., et al., 2012. Reply to 'Constraints on hyperthermals'. Nature Geoscience 5 (4), 231–232.

Davidson, E.A., Janssens, I.A., 2006. Temperature sensitivity of soil carbon decomposition and feedbacks to climate change. Nature 440 (7081), 165–173.

DeConto, R., et al., 2012. Past extreme warming events linked to massive carbon release from thawing permafrost. Nature 484, 87–92.

Dickens, G.R., 2001. Carbon addition and removal during the Late Palaeocene Thermal Maximum: basic theory with a preliminary treatment of the isotope record at ODP Site 1051, Blake Nose. In: Kroon, K., Norris, R.D., Klaus, A. (Eds.), Western North Atlantic Palaeogene and Cretaceous Palaeoceanography. Geological Society Publishing House, Avon, UK, pp. 293–305.

Dickens, G.R., 2003. Rethinking the global carbon cycle with a large, dynamic and microbially mediated gas hydrate capacitor. Earth and Planetary Science Letters 213 (3–4), 169–183.

Dickens, G.R., 2011. Down the Rabbit Hole: toward appropriate discussion of methane release from gas hydrate systems during the Paleocene–Eocene Thermal Maximum and other past hyperthermal events. Climate of the Past 7, 831–846.

Dickens, G.R., O'Neil, J.R., Rea, D.K., Owen, R.M., 1995. Dissociation of oceanic methane hydrate as a cause of the carbon isotope excursion at the end of the Paleocene. Paleoceanography 10 (6), 965–971.

Dickens, G.R., Castillo, M.M., Walker, J.C.G., 1997. A blast of gas in the latest Paleocene; simulating first-order effects of massive dissociation of oceanic methane hydrate. Geology 25 (3), 259–262.

Diefendorf, A.F., Mueller, K.E., Wing, S.L., Koch, P.L., Freeman, K.H., 2010. Global patterns in leaf ^{13}C discrimination and implications for studies of past and future climate. PNAS 107 (13), 5738–5743.

Diefendorf, A.F., Freeman, K.H., Wing, S.L., Graham, H.V., 2011. Production of n-alkyl lipids in living plants and implications for the geologic past. Geochimica et Cosmochimica Acta 75 (23), 7472–7485.

Domingo, L., Lopez-Martinez, N., Leng, M.J., Grimes, S.T., 2009. The Paleocene–Eocene Thermal Maximum record in the organic matter of the Claret and Tendruy continental sections (South-central Pyrenees, Lleida, Spain). Earth and Planetary Science Letters 281, 226–237.

Falkowski, P., et al., 2000. The global carbon cycle: a test of our knowledge of earth as a system. Science 290 (5490), 291–296.

Fang, C., Moncrieff, J.B., 2001. The dependence of soil CO_2 efflux on temperature. Soil Biology and Biochemistry 33 (2), 155–165.

Farley, K.A., Eltgroth, S.F., 2003. An alternative age model for the Paleocene–Eocene Thermal Maximum using extraterrestrial He-3. Earth and Planetary Science Letters 208 (3–4), 135–148.

Friedlingstein, P., et al., 2006. Climate–carbon cycle feedback analysis: results from the C4MIP model intercomparison. Journal of Climate 19 (14), 3337–3353.

Gibbs, S.J., Bown, P.R., Sessa, J.A., Bralower, T.J., Wilson, P.A., 2006a. Nannoplankton extinction and origination across the Paleocene–Eocene Thermal Maximum. Science 314, 1770–1773.

Gibbs, S.J., Bralower, T.J., Bown, P.R., Zachos, J.C., Bybell, L.M., 2006b. Shelf and open-ocean calcareous phytoplankton assemblages across the Paleocene–Eocene Thermal Maximum: implications for global productivity gradients. Geology 34 (4), 233–236.

Giusberti, L., et al., 2007. Mode and tempo of the Paleocene–Eocene Thermal Maximum in an expanded section from the Venetian pre-Alps. Geological Society of America Bulletin 119 (3), 391–412.

Handley, L., Pearson, P.N., McMillan, I.K., Pancost, R.D., 2008. Large terrestrial and marine carbon and hydrogen isotope excursions in a new Paleocene/Eocene boundary section from Tanzania. Earth and Planetary Science Letters 275, 17–25.

Heimann, M., Reichstein, M., 2008. Terrestrial ecosystem carbon dynamics and climate feedbacks. Nature 451.

Higgins, J.A., Schrag, D.P., 2006. Beyond methane: towards a theory for the Paleocene–Eocene Thermal Maximum. Earth and Planetary Science Letters 245 (3–4), 523–537.

Huntzinger, D.N., et al., 2012. North American Carbon Program (NACP) regional interim synthesis: terrestrial biospheric model intercomparison. Ecological Modelling 232, 144–157.

Jackson, S.T., Overpeck, J.T., 2000. Responses of plant populations and communities to environmental changes of the late Quaternary. Paleobiology 26 (4 SUPPS), 194–220.

Jobbagy, E.G., Jackson, R.B., 2000. The vertical distribution of soil organic carbon and its relation to climate and vegetation. Ecological Applications 10 (2), 423–436.

John, C.M., et al., 2008. North American continental margin records of the Paleocene–Eocene Thermal Maximum: implications for global carbon and hydrological cycling. Paleoceanography 23, PA2217.

Kelly, D.C., Nielsen, T.M.J., McCarren, H.K., Zachos, J.C., Röhl, U., 2010. Spatiotemporal patterns of carbonate sedimentation in the South Atlantic: implications for carbon cycling during the Paleocene–Eocene Thermal Maximum. Palaeogeography Palaeoclimatology Palaeoecology 293, 30–40.

Kennett, J.P., Stott, L.D., 1991. Abrupt deep-sea warming, palaeoceanographic changes and benthic extinctions at the end of the Palaeocene. Nature 353 (6341), 225–229.

Kent, D.V., et al., 2003. A case for a comet impact trigger for the Paleocene/Eocene Thermal Maximum and carbon isotope excursion. Earth and Planetary Science Letters 211, 13–26.

King, A.W., Hayes, D.J., Huntzinger, D.N., West, T.O., Post, W.M., 2012. North American carbon dioxide sources and sinks: magnitude, attribution, and uncertainty. Frontiers in Ecology and the Environment 10 (10), 512–519.

Kraus, M.J., Riggins, S., 2007. Transient drying during the Paleocene–Eocene Thermal Maximum (PETM): analysis of paleosols in the Bighorn Basin, Wyoming. Palaeogeography Palaeoclimatology Palaeoecology 245, 444–461.

Kurtz, A.C., Kump, L.R., Arthur, M.A., Zachos, J.C., Paytan, A., 2003. Early Cenozoic decoupling of the global carbon and sulfur cycles. Paleoceanography 18, 1090. http://dx.doi.org/10.1029/2003PA000908.

Magioncalda, R., Dupuis, C., Smith, T., Steurbaut, E., Gingerich, P.D., 2004. Paleocene–Eocene carbon isotope excursion in organic carbon and pedogenic carbonate: direct comparison in a continental stratigraphic section. Geology 32 (7), 553–556.

Mahecha, M.D., Reichstein, M., Carvalhais, N., Lasslop, G., Lange, H., Seneviratne, S.I., Vargas, R., Ammann, C., Arain, M.A., Cescatti, A., Janssens, I.A., Migliavacca, M., Montagnani, L., Richardson, A.D., et al., 2010. Global convergence in the temperature sensitivity of respiration at ecosystem level. Science 329, 838–840.

McCarren, H., Thomas, E., Hasegawa, T., Rohl, U., Zachos, J.C., 2008. Depth dependency of the Paleocene–Eocene carbon isotope excursion: paired benthic and terrestrial biomarker records (Ocean Drilling Program Leg 208, Walvis Ridge). Geochemistry, Geophysics, Geosystems 9 (Q10008(10)).

McInerney, F.A., Wing, S.L., 2011. The Paleocene–Eocene Thermal Maximum: a perturbation of carbon cycle, climate, and biosphere with implications for the future. Annual Review of Earth and Planetary Sciences 39, 489–516.

Muller-Karger, F.E., et al., 2005. The importance of continental margins in the global carbon cycle. Geophysical Research Letters 32 (L01602), 1–4.

Murphy, B.P., Bowman, D.M.J.S., Gagan, M.K., 2007. The interactive effect of temperature and humidity on the oxygen isotope composition of kangaroos. Functional Ecology 21, 757–766.

Murphy, B.H., Farley, K.A., Zachos, J.C., 2010. An extraterrestrial ^{3}He-based timescale for the Paleocene–Eocene Thermal Maximum (PETM) from Walvis Ridge, IODP Site 1266. Geochimica et Cosmochimica Acta 74, 5098–5108.

Nicolo, M.J., Dickens, G.R., Hollis, C.J., 2010. South Pacific intermediate water oxygen depletion at the onset of the Paleocene–Eocene Thermal Maximum as depicted in New Zealand margin sections. Paleoceanography 25, PA4210.

Oberhansli, H., Perch-Nielsen, K., 1990. The Paleocene ^{13}C-event: was it due to changes in the storage rate of terrestrial biomass? Veroff. Ubersee Mus. Bremen Reihe A A10, 99–112.

Pagani, M., Caldeira, K., Archer, D., Zachos, J.C., 2006. An ancient carbon mystery. Science 314, 1556–1557.

Panchuk, K., Ridgwell, A., Kump, L.R., 2008. Sedimentary response to Paleocene–Eocene Thermal Maximum carbon release: a model-data comparison. Geology 36 (4), 315–318.

Prentice, K.C., Fung, I.Y., 1990. The sensitivity of terrestrial carbon storage to climate change. Nature 346 (6279), 48–51.

Röhl, U., Bralower, T.J., Norris, R.D., Wefer, G., 2000. New chronology for the late Paleocene Thermal Maximum and its environmental implications. Geology 28 (10), 927–930.

Röhl, U., Westerhold, T., Bralower, T.J., Zachos, J.C., 2007. On the duration of the Paleocene–Eocene Thermal Maximum (PETM). Geochemistry, Geophysics, Geosystems 8, Q12002.

Sadler, P.M., 1981. Sediment accumulation rates and the completeness of stratigraphic sections. Journal of Geology 89 (5), 569–584.

Schimel, D.S., 1995. Terrestrial ecosystems and the carbon cycle. Global Change Biology 1 (1), 77–91.

Schmitz, B., Pujalte, V., 2003. Sea-level, humidity, and land-erosion records across the initial Eocene Thermal Maximum from a continental–marine transect in northern Spain. Geology 31 (8), 689–692.

Schneider-Mor, A., Bowen, G.J., 2013. Coupled and decoupled responses of continental and marine organic-sedimentary systems through the Paleocene–Eocene Thermal Maximum, New Jersey margin, USA. Paleoceanography 28, 1–11.

Schouten, S., et al., 2007. The Paleocene–Eocene carbon isotope excursion in higher plant organic matter: differential fractionation of angiosperms and conifers in the Arctic. Earth and Planetary Science Letters 258, 581–592.

Schubert, B.A., Jahren, A.H., 2012. The effect of atmospheric CO_2 concentration on carbon isotope fractionation in C_3 land plants. Geochimica et Cosmochimica Acta 96, 29–43.

Schubert, B.A., Jahren, A.H., 2013. Reconciliation of marine and terrestrial carbon isotope excursions based on changing atmospheric CO_2 levels. Nature Communications 4, 1653.

Schulte, P., Scheibner, C., Speijer, R.P., 2011. Fluvial discharge and sea-level changes controlling black shale deposition during the Paleocene–Eocene Thermal Maximum in the Dababiya Quarry section, Egypt. Chemical Geology 285 (1–4), 167–183.

Sluijs, A., Dickens, G.R., 2012. Assessing offsets between the $\delta^{13}C$ of sedimentary components and the global exogenic carbon pool across early Paleogene carbon cycle perturbations. Global Biogeochemical Cycles 26 (4) (GB4005).

Sluijs, A., Bowen, G.J., Brinkhuis, H., Lourens, L.J., Thomas, E., 2007a. The Paleocene–Eocene Thermal Maximum super greenhouse: biotic and geochemical signatures, age models and mechanisms of global change. In: Williams, M., Haywood, A., Gregory, J., Schmidt, D.N. (Eds.), Deep Time Perspectives on Climate Change: Marrying the Signal from Computer Models and Biological Proxies. Geological Society of London. TMS Special Publication, London, pp. 267–293.

Sluijs, A., et al., 2007b. Environmental precursors to rapid light carbon injection at the Palaeocene/Eocene boundary. Nature 1218–1222.

Sluijs, A., et al., 2008a. Eustatic variations during the Paleocene–Eocene greenhouse world. Paleoceanography 23, PA4216.

Sluijs, A., et al., 2008b. Arctic late Paleocene–early Eocene paleoenvironments with special emphasis on the Paleocene–Eocene Thermal Maximum (Lomonosov Ridge, Integrated Ocean Drilling Program Expedition 302). Paleoceanography 23, PA1S11.

Sluijs, A., Zachos, J.C., Zeebe, R.E., 2012. Constraints on hyperthermals. Nature Geoscience 5, 231.

Smith, F.A., Wing, S.L., Freeman, K.H., 2007. Magnitude of the carbon isotope excursion at the Paleocene–Eocene Thermal Maximum: the role of plant community change. Earth and Planetary Science Letters 262, 50–65.

Svensen, H., et al., 2004. Release of methane from a volcanic basin as a mechanism for initial Eocene global warming. Nature 429 (6991), 542–545.
Thomas, D.J., Zachos, J.C., Bralower, T.J., Thomas, E., Bohaty, S., 2002. Warming the fuel for the fire: Evidence for the thermal dissociation of methane hydrate during the Paleocene–Eocene Thermal Maximum. Geology 30 (12), 1067–1070.
Tipple, B.J., et al., 2011. Coupled high-resolution marine and terrestrial records of carbon and hydrologic cycles variations during the Paleocene–Eocene Thermal Maximum (PETM). Earth and Planetary Science Letters 311 (1–2), 82–92.
Trumbore, S., 2000. Age of soil organic matter and soil respiration: radiocarbon constraints on below ground C dynamics. Ecological Applications 10 (2), 399–411.
Walker, J.C.G., Kasting, J.F., 1992. Effects of fuel and forest conservation on future levels of atmospheric carbon dioxide. Global and Planetary Change 97 (3), 151–189.
Westerhold, T., et al., 2008. Astronomical calibration of the Paleocene time. Palaeogeography Palaeoclimatology Palaeoecology 257, 377–403.
Wing, S.L., Harrington, G.J., Bowen, G.J., Koch, P.L., 2003. Floral change during the Initial Eocene Thermal Maximum in the Powder River Basin, Wyoming. In: Wing, S.L., Gingerich, P.D., Schmitz, B., Thomas, E. (Eds.), Causes and Consequences of Globally Warm Climates in the Early Paleogene. Geological Society of America Special Paper, 369. Geological Society of America, Boulder, Colorado, pp. 425–440.
Wing, S.L., et al., 2005. Transient floral change and rapid global warming at the Paleocene–Eocene boundary. Science 310, 993–996.
Zachos, J.C., et al., 2003. A transient rise in tropical sea surface temperature during the Paleocene–Eocene Thermal Maximum. Science 302 (5650), 1551–1554.
Zachos, J.C., et al., 2005. Rapid acidification of the ocean during the Paleocene–Eocene Thermal Maximum. Science 308, 1611–1615.
Zachos, J.C., et al., 2006. Extreme warming of mid-latitude coastal ocean during the Paleocene–Eocene Thermal Maximum: inferences from TEX_{86} and isotope data. Geology 34 (9), 737–740.
Zeebe, R.E., 2012. LOSCAR: long-term ocean–atmosphere–sediment carbon cycle reservoir model v2.0.4. Geoscientific Model Development 5, 149–166.
Zeebe, R.E., Zachos, J.C., 2013. Long-term legacy of massive carbon input to the Earth system: Anthropocene vs. Eocene. Philosophical Transactions of the Royal Society A (in press).
Zeebe, R.E., Zachos, J.C., Dickens, G.R., 2009. Carbon dioxide forcing alone insufficient to explain Palaeocene–Eocene Thermal Maximum warming. Nature Geoscience 2, 576–580.
Zhou, T., Shi, P., Hui, D., Luo, Y., 2009. Global pattern of temperature sensitivity of soil heterotrophic respiration (Q10) and its implications for carbon–climate feedback. Journal of Geophysical Research 114 (G2).